PERGAMON

International Journal of Heat and Mass Transfer 41 (1998) 2837–2846

International Journal of HEAT and MASS TRANSFER

Resonant enhancement of natural convection heat transfer in a square enclosure

Ho Sang Kwak[1,a], Kunio Kuwahara[a], Jae Min Hyun[b]*

[a]*Space Environment Laboratory, The Institute of Space and Astronautical Science, 3-1-1 Yoshinodai, Sagamihara, Kanagawa 229, Japan*

[b]*Department of Mechanical Engineering, Korea Advanced Institute of Science and Technology, 373-1 Kusong-dong, Yusong-gu, Taejon 305-701, South Korea*

Received 8 November 1996

Abstract

A numerical investigation is made of natural convection of an incompressible fluid in a square cavity having a constant-temperature cold sidewall and an opposite hot sidewall with sinusoidally-varying temperature. Comprehensive numerical solutions to the Navier–Stokes equations are acquired for a fixed Rayleigh number and a Prandtl number, $Ra = 10^7$ and $Pr = 0.7$. The amplitude and frequency of the hot wall temperature oscillation are varied. The time-mean heat transfer in the interior as well as the amplifications of fluctuations of instantaneous heat transfer are analyzed. The results disclose that a large-amplitude wall temperature oscillation causes an augmentation of the time-mean heat transfer rate. The maximum gain of the time-mean Nusselt number in the interior occurs at the resonance frequency, at which maximal fluctuations of the Nusselt number are found. The mechanism for resonant enhancement of the time-mean heat transfer is described.

Nomenclature

$A(Nu)$ amplitude of fluctuation of $Nu(t)$, equation (11)
f dimensional frequency of the hot wall temperature oscillation
g gravitational acceleration
$G(Nu)$ gain of the time-mean Nusselt number, equation (10)
L height of the square cavity
N Brunt-Väisäla frequency, $(\alpha g \Delta T/L)^{1/2}$
$Nu(t)$ instantaneous Nusselt number at a vertical plane, equation (9)
$\overline{Nu}$ cycle-averaged value of $Nu(t)$, equations (8) and (9)
p, p^* non-dimensional and dimensional pressures, $p = (p^* + \rho g z^*)L^3/\rho x^2 RaPr$
Pr Prandlt number ν/x
Ra Rayleigh number, $Ra = \alpha g \Delta T L^3/\nu x$
S stratification parameter, $S^2 = \partial\theta/\partial y$
T dimensional temperature
t, t^* non-dimensional and dimensional times, $t = t^*(RaPr)^{1/2}x/L^2$
u, v non-dimensional velocities in x and y directions, $(u, v) = (u^*, v^*)(RaPr)^{-1/2}L/x$
u^*, v^* velocities in x and y directions
x, y non-dimensional horizontal and vertical coordinates, $(x, y) = (x^*, y^*)/L$
x^*, y^* horizontal and vertical coordinates.

Greek symbols
α volumetric expansion coefficient
Δt time increment for numerical calculations
ΔT mean temperature difference between the hot and cold sidewalls, $\bar{T}_h - T_c$
$\Delta T_h'$ amplitude of the hot wall temperature oscillation
Δt time step
Δx grid spacing
ε non-dimensional amplitude of the hot wall temperature oscillation, $\Delta T_h'/\Delta T$
χ thermal diffusivity
ν kinematic viscosity

[1] Current address: Supercomputer Center, Systems Engineering Research Institute, 1 Euen-dong, Yusong, Taejon 305-333, South Korea.

* Corresponding author.

0017–9310/98 $19.00
PII: S0017-9310(98)00018-0

θ non-dimensional temperature, $(T-T_c)/(\bar{T}_h-T_c)$
τ non-dimensional cycle time, $\tau = 2\pi t/\omega$
ω non-dimensional frequency, f/N
ψ non-dimensional stream function, $u = \partial\psi/\partial y$, $v = -\partial\psi/\partial x$.

Subscripts
c cold sidewall
h hot sidewall
i internal gravity wave oscillation
m frequency value at which the maximum $G(Nu)$ occurs
r resonance frequency [at which the maximum $A(Nu)$ occurs]
s steady state solution for the corresponding case with $\varepsilon = 0.0$.

Superscripts
* dimensional quantity
( ) cycle-averaged property, equation (9).

1. Introduction

Natural convection in an enclosure with time-periodic boundary conditions has received much attention in recent years [1–15]. As reviewed by Hyun [16], Fusegi and Hyun [17], and Antohe and Lage [3], the increasing interest is attributable to the relevance of such transient processes in many technological applications. Typical examples are the solar heating varying on a daily basis, and the periodic energizing of electronic devices by the on-and-off heating and/or cooling modes, to name a few.

The main question is how the periodicity of boundary conditions affects the time-dependent flow and associated heat transfer of an enclosed fluid. A practical advantage is that the overall time-averaged heat transfer in the system may be augmented in the case of time-varying boundary conditions as compared with the heat transfer obtained with time-invariant boundary conditions [5–8, 13–15]. Another physically-important aspect of these problems is the possibility of resonance inherent to the system under question [1–7, 12]. Resonance is a phenomenon associated with the eigenmodes of a system, which is essentially independent of the kind of external forcing imposed. If the system is exposed to an external forcing with the correct natural frequency, resonance takes place in which the eigenmodes are excited and amplified.

The numerical work of Lage and Bejan [1] clearly established the presence of resonance in natural convection at high Rayleigh numbers. At one sidewall, a constant temperature was maintained. On the opposite sidewall, a heat flux, which fluctuated in a square-wave fashion, was prescribed. In their problem formulation, resonance was identified by the maximal amplification of fluctuations of the instantaneous Nusselt number at the centerline of the cavity. It was demonstrated numerically that resonance was seen at certain moderate values of frequency. In subsequent papers, Antohe and Lage [3, 4] numerically examined the effects of the Prandtl number and the amplitude of the time-varying heating on the convective transport in a cavity.

Parallel efforts were also made on the experimental front. Antohe and Lage [5] conducted precision-controlled experiments for the problem setup of Lage and Bejan [1]. Attention was focused on the influence of periodic heating on the time-mean heat transfer. For a high Rayleigh number based on the average heat flux, the oscillatory heating led to about 20% augmentation of the time-mean heat transfer coefficient in comparison to that obtained by steady heating with the same time-averaged heat flux. The maximum gain of the time-mean heat transfer was seen at a moderate frequency, which was interpreted to be associated with resonance.

Iwatsu *et al.* [6] investigated convective motions of an incompressible fluid in a cavity with an externally-imposed vertical temperature difference between the top hot endwall and the bottom cold wall. The aim was to explore the enhancement of vertical heat transfer by applying a mechanical oscillation to the top lid. Obviously, the heat transfer in this stably-stratified fluid system would be purely conductive if the top lid is stationary. Numerical results revealed the existence of resonance at particular frequencies of the top lid oscillation. At resonance frequencies, a substantial augmentation of heat transfer and flow fluctuations was demonstrated.

A canonical configuration for confined natural convection is a sidewall-heated cavity [18–20], in which the horizontal heating is provided by a temperature difference applied between two perfectly-conducting vertical sidewalls. Fu and Shieh [7, 8] examined thermal convection which was simultaneously driven by gravity and by the vertical vibration of the cavity. The results disclosed that there exists a resonant convection regime in which the flow and heat transfer interact with the vibration of the gravitational force [7]. For a relatively small Rayleigh number, $Ra = 10^4$, the imposed mechanical vibration produced a substantial augmentation of the overall heat transfer rate at the resonance frequency [7, 8].

The studies of Antohe and Lage [5], Iwatsu *et al.* [6] and Fu and Shieh [7] are strongly suggestive of potentially useful applications. They imply that an external oscillation with properly-chosen frequencies will bring forth the resonance of natural convection, which results in an enhancement of the time-averaged heat transfer rate.

A different type of time-varying conditions has also been taken into account. Yang *et al.* [9] considered a sinusoidally-varying temperature condition on the hot sidewall of a tall rectangular cavity (height : width = 3 : 1). The forcing frequency was fixed and the range of the Rayleigh number was up to 10^6. The effects of frequency and amplitude of sidewall temperature oscillation in a square cavity were examined by Kazmierczak

and Chinoda [10], for a fixed Rayleigh number 1.4×10^5. However, these works did not detect resonance because of the limited ranges of principal parameters covered; in particular, the Rayleigh number was too low. Xia *et al.* [11] examined the same problem for high Rayleigh numbers. The impacts of the wall temperature oscillation on the flow stability were elucidated, but the frequency was set at a fixed value. The possibility of resonance was not a key issue in these investigations.

Recently, Kwak and Hyun (hereinafter referred to as KH, [12]) performed comprehensive numerical computations for the same problem formulation as adopted by Kazmierczak and Chinoda [10]. The numerical solutions encompassed a broad range of frequency, and the results clearly illustrated the presence of resonance. The fluctuations of the Nusselt number were substantially amplified by the periodically-varying temperature condition with the proper resonance frequency. The physical mechanism of resonance was delineated by examining the evolutions of detailed flow and temperature fields over a cycle. Quantitative comparisons were conducted for the resonance frequency between the numerical results and the available theoretical predictions. The results show that the flow in this configuration resonates to the internal gravity-wave oscillations.

It is to be noted that, in the studies of KH [12], the amplitude of the temperature oscillation imposed at the sidewall was set to be small. They used the non-dimensional amplitude $\varepsilon = 0.1$, which implies that the amplitude of temperature oscillation at the boundary wall was 10% of the mean temperature difference between the two sidewalls. Because of this constraint, the cycle-averaged flow and temperature fields do not deviate much from those of the corresponding non-oscillating case with the same time-mean value. In the present study, the basic analysis of KH [12] is extended to the cases when the amplitude of the temperature oscillation at the boundary wall is finite. The aim is to explore the changes in time-averaged heat transfer rate in the cavity especially when the external thermal forcing is applied at the proper resonance frequency. In order to focus on the effects of amplitude of the external thermal forcing, numerical solutions are obtained for values of ε up to $\varepsilon = 1.0$ with Ra and Pr fixed. A large value of Ra, $Ra = 10^7$, is chosen. Guided by the earlier studies [5, 12], Pr is selected to be $O(1)$, which has been known to give rise to pronounced results of resonance. It is shown that, as observed in the prior investigations [5–8], the time-averaged heat transfer in the present configuration is altered appreciably by an application of large-amplitude oscillatory thermal forcings at the boundary.

2. The numerical model

Consider a square cavity filled with an incompressible Boussinesq fluid having constant physical properties. The top and bottom horizontal walls are thermally insulated. The left sidewall is kept at a constant temperature T_c. The temperature at the right sidewall, T_h, varies with time at $T_h = \bar{T}_h + \Delta T_h' \sin(ft^*)$, where $\Delta T_h'$ and f are respectively the amplitude and frequency of the hot wall temperature oscillation. The mean temperature difference between the two sidewalls, $\Delta T = \Delta \bar{T}_h - T_c$, is positive and constant. The flow configuration is schematically described in Fig. 1. The time-varying thermal boundary condition at the hot vertical wall is depicted in Fig. 2.

The governing equations are the two-dimensional Navier–Stokes equations for a Boussinesq fluid. These, in nondimensional form, are expressed as

$$\frac{\partial u}{\partial t} + \frac{\partial}{\partial x}(u^2) + \frac{\partial}{\partial y}(uv) = -\frac{\partial p}{\partial x} + \left(\frac{Pr}{Ra}\right)^{1/2}\left(\frac{\partial^2 u}{\partial x^2} + \frac{\partial^2 u}{\partial y^2}\right) \tag{1}$$

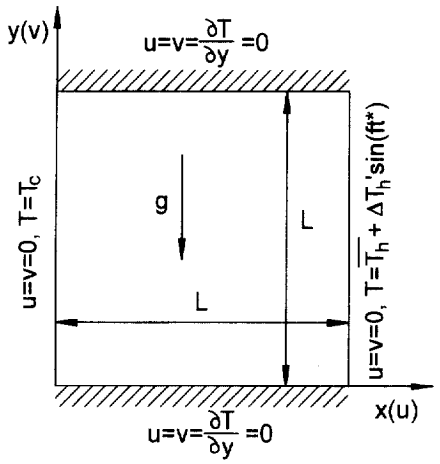

Fig. 1. Schematic diagram of the flow configuration.

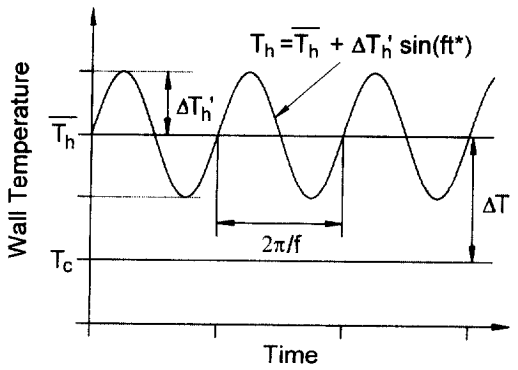

Fig. 2. Time-dependent temperature boundary conditions at the vertical sidewalls.

$$\frac{\partial v}{\partial t}+\frac{\partial}{\partial x}(uv)+\frac{\partial}{\partial y}(v^2) = -\frac{\partial p}{\partial y}+\theta+\left(\frac{Pr}{Ra}\right)^{1/2}\left(\frac{\partial^2 v}{\partial x^2}+\frac{\partial^2 v}{\partial y^2}\right) \quad (2)$$

$$\frac{\partial \theta}{\partial t}+\frac{\partial}{\partial x}(u\theta)+\frac{\partial}{\partial y}(v\theta) = \left(\frac{1}{PrRa}\right)^{1/2}\left(\frac{\partial^2 \theta}{\partial x^2}+\frac{\partial^2 \theta}{\partial y^2}\right) \quad (3)$$

$$\frac{\partial u}{\partial x}+\frac{\partial v}{\partial y}=0. \quad (4)$$

In the above, non-dimensionalization was effectuated by using L, NL and, $1/N$ as reference scales for length, velocity, time, respectively. Here, N is the Brunt-Väisälä frequency, i.e., $N^2 \equiv \alpha g \Delta T/L$. The temperature was non-dimensionalized as $\theta=(T-T_c)/\Delta T$. The relevant dimensionless parameters are the Rayleigh number, $Ra=\alpha g \Delta T L^3/\nu x$; the Prandtl number, $Pr=\nu/x$; the non-dimensional amplitude of thermal forcing, $\varepsilon=\Delta T_h/\Delta T$; and the non-dimensional frequency, $\omega=f/N$.

The boundary conditions are

$$u=v=\frac{\partial \theta}{\partial y}=0 \quad \text{at } y=0,1 \quad (5)$$

$$u=v=\theta=0 \quad \text{at } x=0 \quad (6)$$

$$u=v=0 \quad \theta=1+\varepsilon\sin(\omega t) \quad \text{at } x=1. \quad (7)$$

A finite-volume procedure based on the SIMPLER algorithm [21] was employed to solve the system of equations (1)–(4). The numerical accuracy of the present method is $O(\Delta t, \Delta x^2)$, where Δt and Δx are the time step and grid spacing. The present numerical model was verified by reproducing the results of Lage and Bejan [1] and other benchmark configurations. The numerical methodologies were described in detail in KH [12].

For all the computations, a grid with (82×62) mesh points in the $(x\times y)$ domain was used. Grid stretching was performed to resolve thin boundary layers on the solid walls. A small time step, $\Delta t=2\pi/(1024\omega)$, i.e., 1024 time steps per cycle, was used. Extensive convergence tests were carried out, and the robustness of the present code has been established [12].

In actual computations, a steady state solution was acquired for a corresponding non-oscillating case ($\varepsilon=0$), which is referred to as the basic state. This solution was used as the initial condition in simulating the cases of time-varying temperature conditions ($\varepsilon\neq 0$). This approach was adopted by previous works [1–4, 12], which resulted in saving a considerable amount of computation time.

Numerical computations were conducted for $\varepsilon=0.1$, 0.5, and 1.0 with fixed values of Ra and Pr, i.e., $Ra=10^7$ and $Pr=0.7$. The frequency of the wall temperature oscillation encompassed the range $0.1\leqslant\omega\leqslant 1.5$. Guided by the earlier study [12], attention was focused to the frequency band near the expected resonance frequency.

Here, it is advantageous to introduce several operators. The mean value $\bar{\phi}$ of an oscillating property $\phi(t)$ over a cycle can be written as

$$\bar{\phi}=\frac{\omega}{2\pi}\int_{t_0}^{t_0+2\pi/\omega}\phi(t)\,dt. \quad (8)$$

The instantaneous Nusselt number, $Nu(t)$, averaged over the vertical plane at $x=a$, is obtained as

$$Nu(t)_{x=a}=\int_0^1\left[\frac{\partial\theta}{\partial x}-u\theta(RaPr)^{1/2}\right]_{x=a}dy. \quad (9)$$

The positive sign of $Nu(t)_{x=a}$ implies that the heat is transported from the right part to the left part relative to the vertical plane $x=a$. In order to assess the impact of the wall temperature oscillation on the heat transfer characteristics, the following definitions are made

$$G(Nu)=\frac{\overline{Nu}-Nu_s}{Nu_s} \quad (10)$$

$$A(Nu)=\frac{\text{Max}\{Nu(t)\}-\text{Min}\{Nu(t)\}}{Nu_s} \quad \text{for } t_0\leqslant t\leqslant t_0+\frac{2\pi}{\omega}. \quad (11)$$

It is recalled that Nu_s denotes the corresponding value of Nu in the case of non-oscillating wall temperature ($\varepsilon=0$), which is $Nu_s[\equiv Nu(t=0)]$ in the present numerical procedure. $G(Nu)$ and $A(Nu)$ represent the gain and the fluctuating amplitude of heat transfer relative to the corresponding non-oscillating value, respectively. The values of $G(Nu)$ and $A(Nu)$ are estimated by using solution during a cycle after the approximate steady periodic state has been reached.

In the present study, that the values of $Nu(t)$ are estimated at the hot wall, at the cold wall, and at the vertical plane ($x=0.5$). For the basic-state solution ($\varepsilon=0$), heat balance (difference between the hot and cold wall Nusselt numbers) is satisfied within $O(10^{-6})$. In the case of oscillating wall temperature, the values of Nu estimated at the above three different positions show agreement with 1% relative error.

3. Results and discussion

Figure 3 depicts the temporal behavior of $Nu(t)$ at the vertical mid-plane $x=0.5$. For all the cases, $Nu(t)$ settles down to a quasi-steady periodic form after several cycles. Figure 3(a) shows the results for $\varepsilon=0.1$. The fluctuation of $Nu(t)$ at a moderate frequency ($\omega=0.67$) is far more pronounced in comparison with the cases of small ($\omega=0.4$) and large ($\omega=1.0$) frequencies. This points to the presence of resonance. Following the previous arguments of Lage and Bejan [1] and KH [12], the resonance can be identified by maximal amplification of fluctuation of $Nu(t)_{x=0.5}$ at a certain specific frequency (referred to as the resonance frequency ω_r). The results

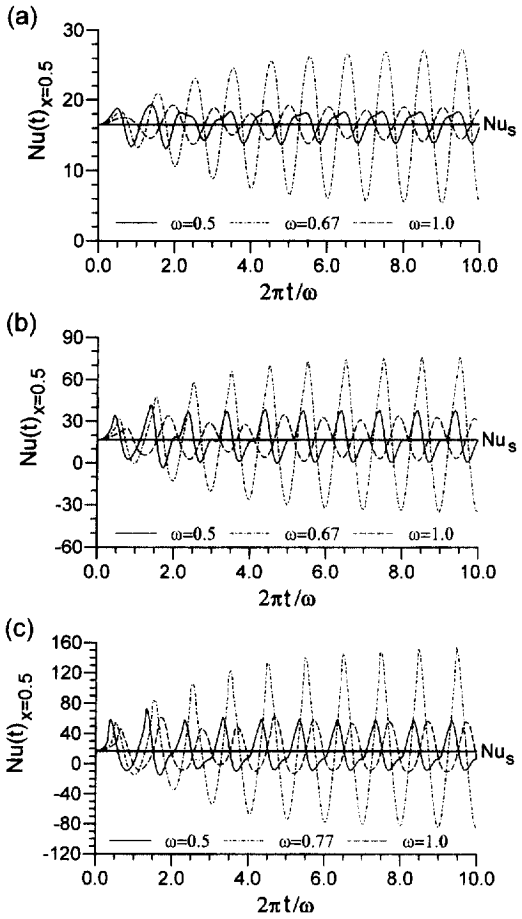

Fig. 3. Time-dependent behavior of the Nusselt number at the vertical mid-plane ($x = 0.5$). (a) $\varepsilon = 0.1$; (b) $\varepsilon = 0.5$; (c) $\varepsilon = 1.0$.

for larger amplitudes $\varepsilon = 0.5$, 1.0 are displayed in Figs. 3(b) and 3(c). The qualitative behavior of oscillation of $Nu(t)$ is generally similar to that for $\varepsilon = 0.1$. However, quantitative differences are ostensible; the fluctuating amplitude of $Nu(t)$ becomes substantially larger as ε increases from 0.1 to 1.0.

The effects of ε and ω on the fluctuation of $Nu(t)$ at $x = 0.5$ are scrutinized in Fig. 4, in which existence of resonance is discernible. For the three values of ε, the curves of the normalized amplitude $A(Nu)/\varepsilon$ exhibit the sharp resonance peaks. The values of the resonance frequency, ω_r, at which the maximum $A(Nu)$ occurs, are listed in Table 1.

An interesting finding in Fig. 4 is that $A(Nu)$ displays a similar parametric dependence on ω. It is noticeable that the $A(Nu)/\varepsilon$ vs. ω curves for the three values of ε exhibit a very similar trend. The results for $\varepsilon = 0.1$ and $\varepsilon = 0.5$ disclose that the influence of ε on $A(Nu)/\varepsilon$ is found to be insignificant. Put it alternatively, $A(Nu)$ is approximately proportional to ε when ε is small. This is in line with the theoretical prediction of Antohe and Lage [3] that the resonance amplitude of the Nusselt number is a nearly-linear function of the amplitude of the applied heat flux. Small differences are seen when ε is large.

The present results are consistent with the general discussion on the issue of the superposing oscillation on a steady basic flow. In a system without damping, any periodic excitation with the correct natural frequencies of the system would give rise to an oscillation with infinite amplitude. In the presence of damping, the amplification

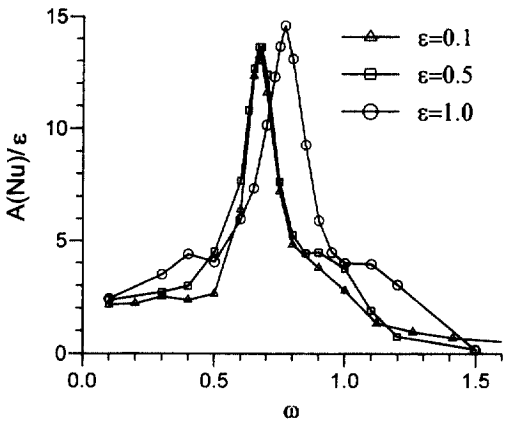

Fig. 4. Effects of ε on the $A(Nu)/\varepsilon$ variation with ω ($x = 0.5$).

Table 1
Summary of the present numerical simulations

		$\varepsilon = 0.0$	$\varepsilon = 0.1$	$\varepsilon = 0.5$	$\varepsilon = 1.0$
Maximum amplification of fluctuation of	$A(Nu)$	0.0	0.662	3.40	7.29
$Nu(t)$ at $x = 0.5$ (Fig. 4)	ω_r	—	0.67	0.67	0.77
Maximum gain of $\overline{Nu}$ (Fig. 5)	$G(Nu)$	0.0	0.00213	0.0421	0.131
	ω_m	—	0.68	0.65	0.77
Estimated values from the cycle-averaged	S^2	0.880	0.884	0.920	1.17
solutions [Fig. 9 and equation (12)]	ω_i	0.66	0.66	0.68	0.76

characteristics are controlled mainly by the damping mechanism of the system. In the present calculations, Ra and Pr are fixed, i.e., the viscous and diffusive dampings are constrained. If ε is sufficiently small so that the effect of the superimposed oscillations is linear, the resulting amplification is linearly proportional to ε, without affecting f_r. However, when ε becomes large, nonlinear behavior is manifest and it distorts both $A(Nu)$ and f_r. All these behaviors are shown in the present results.

Next, the effect of ε on the time-mean heat transfer rate is described. A careful inspection of Fig. 3(c) discloses that the temporal behavior of $Nu(t)$ at $\omega = 0.77$ is almost sinusoidal but not symmetric about the value of Nu_s. This is indicative of the fact that Nu deviates from the corresponding value of the non-oscillating case. In order to confirm this assertion, the values of $G(Nu)/\varepsilon$ at $x = 0.5$ are plotted versus ω in Fig. 5. For $\varepsilon = 0.1$, Nu remains almost unchanged from Nu_s at all frequencies. As remarked by KH [12], the overall time-mean characteristics of natural convection remain substantially unchanged by the sidewall temperature oscillation when the amplitude of forcing is small. However, as ε increases, the effect of ε on Nu becomes conspicuous. When ε is appreciable, $G(Nu)$ increases with ε in a nonlinear manner (note that in the ordinate $G(Nu)/\varepsilon$ is plotted). As shown, the time-mean heat transfer rate is augmented measurably when the wall temperature oscillates with a large amplitude. The maximum gain of Nu relative to Nu_s is approximately 4.2% (for $\varepsilon = 0.5$) and 13.1% (for $\varepsilon = 1.0$).

The dependency of $G(Nu)$ on ω is also illustrated in Fig. 5. For small ω, $G(Nu)$ has an almost constant but finite positive value; e.g., $G(Nu) = 0.0866$ for $\varepsilon = 1.0$ and $\omega = 0.1$. When $\omega \ll \omega_r$, the impacts of wall temperature oscillation can penetrate the full cavity [8, 10]. In this case, the periodic responses of natural convection can be deduced from a series of steady state solutions, each of which may be computed with a constant hot wall temperature in the range of $1-\varepsilon \leqslant \theta_h \leqslant 1+\varepsilon$. When the amplitude of forcing is small, $\varepsilon \ll 1$, the time-dependent flow and heat transfer exhibit oscillatory behavior which is almost symmetric about the basic state solution ($\varepsilon = 0$). However, when ε is large, this argument is no longer valid. It is worth noting that the amount of heat transported by natural convection from the hot wall to the cold wall does not vary linearly with the temperature difference between the two sidewalls. Consequently, the fluctuation of $Nu(t)$ is not symmetric about Nu_s. These considerations offer plausible physical explanations for the deviation of Nu from Nu_s at small frequencies (see, e.g., Antohe and Lage [5]).

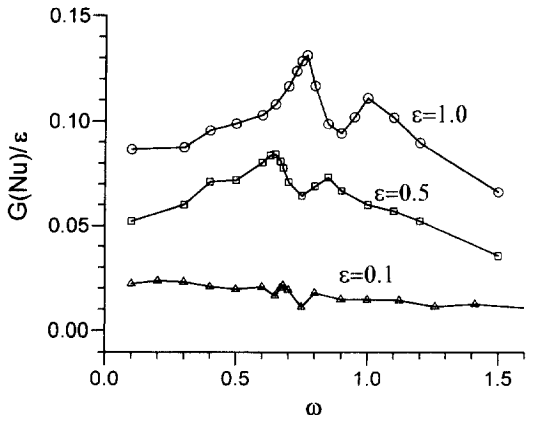

Fig. 5. Effects of ε on the $G(Nu)/\varepsilon$ variation with ω ($x = 0.5$).

On the other hand, as ω increases beyond ω_r, $G(Nu)$ decreases with ω. As stressed in the previous works [8, 10, 12], when $\omega \gg 1$, the direct effects of the wall temperature oscillation are confined to the vertical boundary layer on the hot sidewall; the fluid in the interior does not feel the presence of the hot wall temperature oscillation. Thus, the deviation of Nu from Nu_s is small. The $G(Nu)-\omega$ curves in Fig. 5 exhibit a secondary peak at a frequency which is larger than ω_r. Since the presence of a secondary peak is not clearly discernible in the $A(Nu)-\omega$ curves in Fig. 4, this peak can not be interpreted conclusively as the existence of another distinct frequency of the system. This issue should be examined in detail in the forthcoming investigations.

It is important to note that the maximum gain of time-mean heat transfer occurs at a moderate frequency in a band near the resonance frequency, ω_r. The values of the frequency at which the maximum $G(Nu)$ takes place, ω_m, are listed in Table 1. The present result is supportive of the assertion that the maximal gain of the time-mean heat transfer coefficient, which is observed at a moderate frequency, is interpreted to be a consequence of resonance.

Another effect of large ε can be found in Figs. 3(a) and 3(b); when ε is large, $Nu(t)$ becomes negative at some instant during a cycle. In order to make a physical interpretation of this result, the $A(Nu)$ vs. ω curves for $\varepsilon = 1.0$ are shown in Fig. 6 at three representative locations, i.e., at the cold sidewall ($x = 0.0$), at the vertical mid-plane ($x = 0.5$), and at the hot sidewall ($x = 1.0$).

The value of $A(Nu)/2$ at the cold wall is less than unity, and this is smaller than $A(Nu)/2$ at the hot wall and at the vertical mid-plane. Considering that $G(Nu) \sim O(10^{-1})$, heat is always transferred out of the cavity at the cold wall. On the other hand, the value of $A(Nu)/2$ at the hot wall is much greater than unity. Put it alternately, the instantaneous values of $Nu(t)$ can be negative. This again implies that heat is instantaneously transferred either into the cavity or out of the cavity at the hot wall during a cycle. Here, it is useful to follow the descriptions of KH [12]; a cycle can be divided into the cooling ($\theta_h < 1.0$) and heating ($\theta_h > 1.0$) phases at the hot wall *relative* to

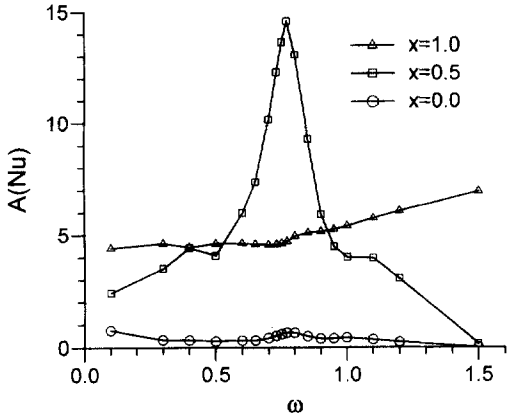

Fig. 6. Variation of $A(Nu)$ vs. ω at three locations, $x = 0$, $x = 0.5$ and $x = 1.0$. $\varepsilon = 1.0$.

the mean temperature ($\overline{\theta_h} = 1.0$). The negative value of $Nu(t)$ at the hot wall can occur when the hot wall temperature becomes lower than the fluid temperature in the thermal boundary layer in the cooling phase. When $\varepsilon = 0$, the fluid releases thermal energy fully to the cold wall. However, when $\varepsilon > 0$, there exists another choice in that thermal energy is partially returned to the hot wall in the relative cooling phase. The difference between the Nusselt numbers at the hot and cold walls is indicative of the transient thermal storage capacity of the system (see, e.g., Antohe and Lage [2]). As illustrated in Fig. 6 as well as in KH [12], $A(Nu)_{x=1}$ increases with ε and ω, i.e., the latter mechanism tends to outweigh the former. In this case, the system has the capacity to store thermal energy in transient states.

It is also discernible that $A(Nu)$ at $x = 0.5$ has a peak value at $\omega = \omega_r$, which is much larger than $A(Nu)$ at the cold wall and at the hot wall. As a result, the Nusselt number at $x = 0.5$, has a negative value of very large absolute magnitude at some time instance, as shown in Fig. 3(c). The fluid in the cavity experiences the heat transport from the left half domain to the right half domain and vice versa periodically during a cycle. However, the occurrence of negative value of $Nu(t)$ in the interior has a different origin; it is of convective nature. The maximal amplification of $Nu(t)$ at $x = 0.5$ is closely associated with maximal fluctuations of the flow at $\omega = \omega_r$. In particular, the negative value of $Nu(t)$ at $x = 0.5$ take places when the clockwise (CW) flow circulations are developed, which will be shown later.

The discussion will now be centered on the resonance cases. In order to acquire a physical insight into resonance, detailed descriptions of the evolutions of flow and temperature fields over a cycle are needed, as displayed in Figs. 7 and 8.

Figure 7 depicts the time-dependent flow patterns in the periodic steady state over a cycle for $\varepsilon = 1.0$ and $\omega = 0.77$. The sequential growth and disappearance of the counterclockwise (CCW) and clockwise circulations in a cycle are discernible. The CW and CCW circulations represent the influences of the relative cooling and heating phases, respectively. During the relative heating phase in Fig. 7 ($19 \leqslant \tau \leqslant 19.5$), the CCW circulations are intensified with time, and the maximum strength of flow occurs near the time instant at which the relative heating has been fully accomplished. During the relative cooling phase ($19.5 \leqslant \tau \leqslant 20$), the reverse process takes place.

Here, it is pointed out that the CW circulations as well as the CCW circulations grow to fill the bulk of the cavity, as shown in Fig. 7(a). It is noted that, for the case of $\varepsilon = 0.1$, the CCW circulations dominate in the cavity at all time instants. When ε is small, the fluctuating components of the flow are overshadowed by the global flow driven by the mean temperature difference between the two sidewalls [12]. However, for $\varepsilon = 1.0$, the flow fluctuations at the resonance frequency are comparable to the flow sustained by the mean temperature difference between the two sidewalls. Consequently, the wall temperature oscillation with a large amplitude causes a substantial amplification of flow, therefore, the instantaneous flow differs much from the basic state.

Sequential plots showing the evolutions of temperature field over a cycle are depicted in Fig. 8. It is obvious that the isotherms in the interior exhibit a periodic tilting over a cycle. This temporal behavior of the interior fluid was previously reported by KH [12], although the degree of tilting was smaller due to a small value of ε ($\varepsilon = 0.1$) used in [12]. This suggests that the resonance is associated with the internal gravity wave modes. It also reinforces the earlier assertion that the mechanism of resonance is largely independent of the forcing amplitude.

The influences of a large amplitude ($\varepsilon = 1.0$) are exemplified in Fig. 8. The regions of $\theta > 1.0$ are seen in the upper part of the cavity at all times throughout a cycle. This implies that the cycle-averaged temperature field deviates much from that for the case of non-oscillating hot-wall temperature ($\varepsilon = 0.0$). Figures 7 and 8 demonstrate that both the time-mean solutions and the instantaneous solutions are affected much by the wall-temperature oscillation when ε is large.

The time-mean flow patterns and temperature fields are acquired by averaging the time-dependent solutions over a cycle, which are illustrated in Fig. 9. Differences between the time-mean solution for $\varepsilon = 0.1$ and the basic state solution ($\varepsilon = 0.0$) are hardly discernible. This again supports the assertion of KH [12] that the impacts of wall temperature oscillation of small amplitude on the time-mean solutions are meager. However, for $\varepsilon = 0.5$, both the flow and temperature fields display noticeable changes from the basic state. For $\varepsilon = 1.0$, the deviations from the basic state are pronounced. In particular, the structure of flow and temperature fields in the interior, rather than in the boundary layers, is significantly

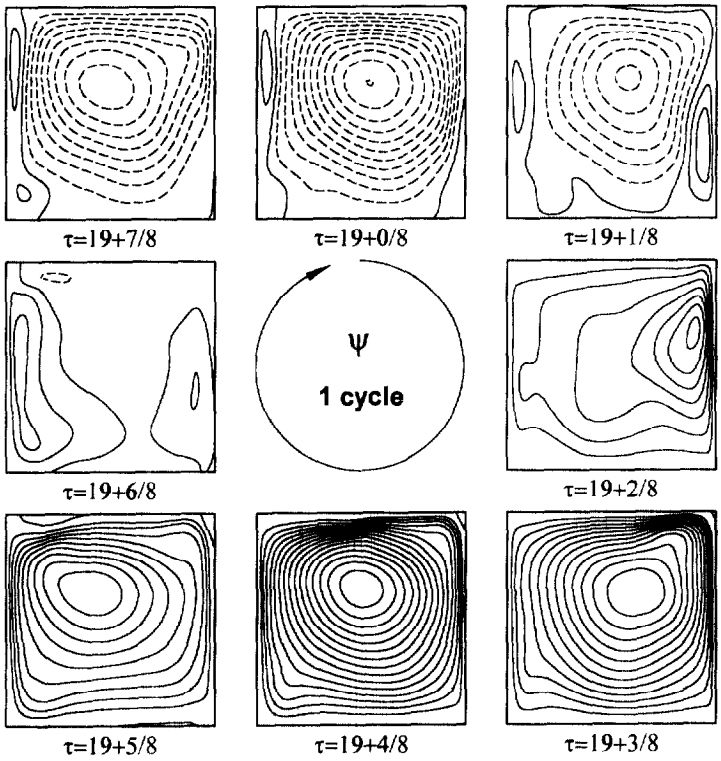

Fig. 7. Sequential plots showing the periodic stream functions in a cycle. $\varepsilon = 1.0$, $\omega = 0.77$. The time instants, $\tau(=2\pi t/\omega)$, are given in the figures. The contour increments are $\Delta\psi = 0.004$. The dashed lines indicate the negative contour values.

changed. This, of course, is the case with a large value of ε. As mentioned before, when ε is large, the time-varying responses of flow and temperature fields in a cycle are no longer symmetric about the basic state. The asymmetric characteristics manifest the differences of the cycle-averaged time-mean solution from the basic state. These lead to the enhancement of the time-mean heat transfer rate.

When ε is large (see Fig. 4 for $\varepsilon = 1.0$), the departure of the time-mean temperature field from the basic state provides a plausible explanation for the shift of the resonance frequency toward a larger value. The present results shown in Figs. 4–8 are consistent with the previous finding of KH [12] that the flow resonates with the internal gravity wave oscillations. For the present configuration, Paolucci and Chenoweth [19] estimated the frequency of the internal wave modes. The frequency of the fundamental mode can be expressed, in the present non-dimensionalization scheme, as

$$\omega_i = \frac{S}{\sqrt{2}} \tag{12}$$

where $S^2(\equiv \partial\theta/\partial y)$ is a parameter indicating the overall strength of stratification.

KH [12] estimated the stratification factor S of the basic state by using a linear fitting to the vertical temperature distribution at the horizontal mid-width plane of the cavity ($x = 0.5$). The predicted values of ω_i were in good agreement with the numerically-acquired values of ω_r. In this study, S is obtained from the cycle-averaged solutions, rather than the basic state; S is evaluated by using the temperature profile in the range $0.2 \leqslant y \leqslant 0.8$ on the vertical plane at $x = 0.5$. This reflects the fact that, when ε is large, the time-mean temperature field differs appreciably from the basic state. The estimated values of S and ω_i are listed in Table 1. It is seen that $\omega_i \approx \omega_r \approx \omega_m$. The slightly larger value of the resonance frequency for $\varepsilon = 1.0$ is a consequence of the fact that the time-mean temperature field is more strongly stratified, therefore, the frequency of internal gravity mode has a slightly larger value.

4. Conclusion

Numerical computations have been conducted for natural convection in a sidewall-heated cavity with a time-varying temperature at the hot sidewall, $\theta_h = 1 + \varepsilon\sin(\omega t)$. The effects of amplitude of the wall temperature oscillation on the time-mean heat transfer and the amplifications of fluctuations of the instantaneous heat transfer are investigated.

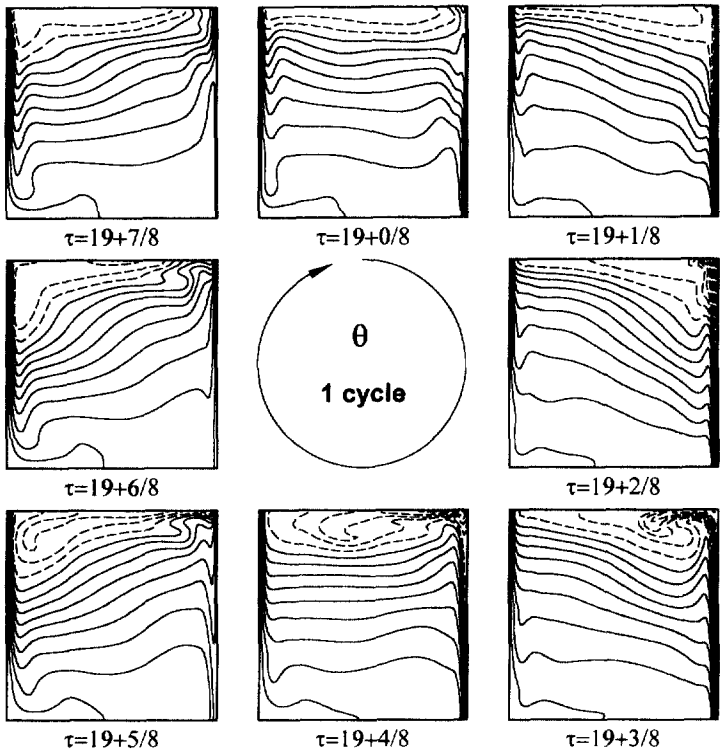

Fig. 8. Same as in Fig. 7 except for contour plots of isotherms. $\Delta\theta = 0.1$. The dashed lines indicate the contour values $\theta \geqslant 1.0$.

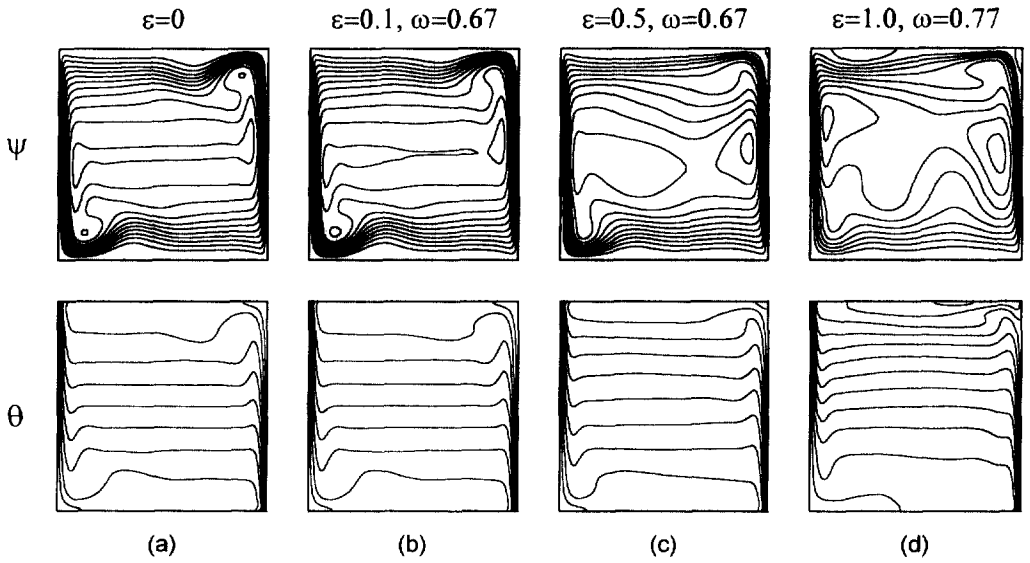

Fig. 9. Contour plots of stream functions (upper frames) and isotherms (lower frames) (a) of the basic-state solution, and (b)–(d) of the cycle-averaged solutions. $\Delta\psi = 0.001$ and $\Delta\theta = 0.1$.

The amplification characteristics of the fluctuation of the heat transfer in the interior are linearly dependent on ε when ε is small. When ε is large, the time-mean heat transfer is augmented measurably from the corresponding value for the case of the non-oscillating temperature condition ($\varepsilon = 0.0$). The maximum gain of the time-mean heat transfer rate is seen at the resonance frequency at which maximal fluctuation of heat transfer takes place. This suggests that the augmentation of time-mean heat transfer is a consequence of resonance.

Although the influences of ε are discernible both in the time-mean and instantaneous flow and temperature fields, the basic mechanism of resonance is largely independent of the amplitude of thermal forcing. The evolutions of flow and temperature fields over a cycle and the theoretical predictions based on the analyses of the cycle-averaged temperature fields indicate that the flow resonates with the internal gravity-wave oscillations.

In this study, attention is limited to the special case of $Ra = 10^7$ and $Pr = 0.7$ to concentrate on the amplitude effect on the time-mean heat transfer. Due to the sensitivity of the natural convection to inertial effects, the cases with different Ra and Pr will be of interest. Another restriction is that the present study is performed under the Boussinesq-fluid approximation, which may not be valid in the case of large ε or ΔT. It is also stressed that the non-Boussinesq effects are known to influence the oscillatory modes of the basic-state flow. Subsequent efforts to resolve these issues are being planned for future work.

Acknowledgements

Appreciation is extended to the referees who provided constructive comments and suggestions. This work was supported in part by a grant from the Center of Excellence (COE) Program of the Ministry of Education, Science, Sports and Culture, Japan.

References

[1] Lage JL, Bejan A. The resonance of natural convection in an enclosure heated periodically from the side. Int J Heat Mass Transfer 1993;36:2027–38.

[2] Antohe BV, Lage JL. A dynamic thermal insulator: inducing resonance within a fluid saturated porous medium enclosure heated periodically from the side. Int J Heat Mass Transfer 1994;37:771–82.

[3] Antohe BV, Lage JL. Amplitude effect on convection induced by time-periodic horizontal heating. Int J Heat Mass Transfer 1996;38:1121–33.

[4] Antohe BV, Lage JL. The Prandtl number effect on the optimum heating frequency of an enclosure filled with fluid or with a saturated porous medium. Int J Heat Mass Transfer 1997;40:1313–23.

[5] Anothe BV, Lage JL. Experimental investigation on pulsating horizontal heating of an enclosure filled with water. ASME J Heat Transfer 1996;118:889–96.

[6] Iwatsu R, Hyun JM, Kuwahara K. Convection in a differentially-heated square cavity with a torsionally-oscillating lid. Int J Heat Mass Transfer 1992;35:1069–76.

[7] Fu WS, Shieh WJ. A study of thermal convection in an enclosure induced simultaneously by gravity and vibration. Int J Heat Mass Transfer 1992;35:1695–710.

[8] Fu WS, Whieh WJ. Transient thermal convection in an enclosure induced simultaneously by gravity and vibration. Int J Heat Mass Transfer 1993;36:437–52.

[9] Yang HQ, Yang KT, Xia Q. Periodic laminar convection in a tall vertical cavity. Int J Heat Mass Transfer 1989;32:2199–207.

[10] Kazmierczak M, Chinoda Z. Buoyancy-driven flow in an enclosure with time-periodic conditions. Int J Heat Mass Transfer 1992;35:1507–18.

[11] Xia Q, Yang KT, Mukutmoni D. Effect of imposed wall temperature oscillations on the stability of natural convection in a square enclosure. ASME J Heat Transfer 1995;117:113–20.

[12] Kwak HS, Hyun JM. Natural convection in an enclosure having a vertical sidewall with time-varying temperature. J Fluid Mech 1996;329:65–88.

[13] Kazmierczak M, Muley A. Steady and transient natural convection experiments in a horizontal porous layer. The effects of a thin top fluid layer and oscillating bottom wall temperature. Int J Heat Fluid Flow 1994;15:30–41.

[14] Mantle J, Kazmierczak M, Hiawy B. The effect of temperature modulation on natural convection in a horizontal layer heated from below: high Rayleigh number experiments. ASME J Heat Transfer 1994;116:614–20.

[15] Lage JL. Convective currents induced by periodic time-dependent density gradient. Int J Heat Fluid Flow 1994;15:233–40.

[16] Hyun JM. Unsteady buoyant convection in an enclosure. Advances in Heat Transfer 1994;34:277–320.

[17] Fusegi T, Hyun JM. Laminar and transitional natural convection in an enclosure with complex and realistic conditions. Int J Heat Fluid Flow 1994;15:258–68.

[18] Patterson J, Imberger J. Unsteady natural convection in a rectangular cavity. J Fluid Mech 1980;54:417–21.

[19] Paolucci S, Chenoweth DR. Transition to chaos in a differentially heated vertical cavity. J Fluid Mech 1989;215:379–410.

[20] Quere Le. Transition to unsteady natural convection in a tall water-filled cavity. Phys Fluids A 1990;2:503–14.

[21] Patankar SV. Numerical Heat Transfer and Fluid Flow, New York: McGraw-Hill, 1980.